Construction of a Deformable Spatiotemporal MRI Atlas of the Fetal Brain: Evaluation of Similarity Metrics and Deformation Models

Ali Gholipour[1], Catherine Limperopoulos[2], Sean Clancy[1], Cedric Clouchoux[2], Alireza Akhondi-Asl[1], Judy A. Estroff[1], and Simon K. Warfield[1]

[1] Department of Radiology, Boston Children's Hospital, and Harvard Medical School, 300 Longwood Ave., Boston, MA 02115, USA
[2] Children's National Medical Center, Washington DC, USA

Abstract. The development and identification of best methods in fetal brain MRI analysis is crucial as we expect an outburst of studies on groupwise and longitudinal analysis of early brain development in the upcoming years. To address this critical need, in this paper, we have developed a mathematical framework for the construction of an unbiased deformable spatiotemporal atlas of the fetal brain MRI and compared it to alternative configurations in terms of similarity metrics and deformation models. Our contributions are twofold: first we suggest a novel approach to fetal brain spatiotemporal atlas construction that shows high capability in capturing anatomic variation between subjects; and second, within our atlas construction framework we evaluate and compare a set of plausible configurations for inter-subject fetal brain MRI registration and identify the most accurate approach that can potentially lead to most accurate results in population atlas construction, atlas-based segmentation, and group analysis. Our evaluation results indicate that symmetric diffeomorphic deformable registration with cross correlation similarity metric outperforms other configurations in this application and results in sharp unbiased atlases that can be used in fetal brain MRI analysis.

1 Introduction

Recent advances in volumetric fetal brain MRI reconstruction [1,2,3] have led to new advances in computational analysis of fetal brain MRI including atlas construction, automatic fetal brain MRI segmentation, and group analysis [4,5,6,7,8,9]. Inter-subject image registration is a fundamental component of many of these studies. Precise, topology-preserving image registration, if achieved, can be used to generate optimal unbiased atlases of the anatomy and reliable segmentations of the brain tissue and structures when precise atlas labels are available. This is particularly important in the analysis of early developing brain which undergoes rapid changes in anatomy due to complex growth processes. Inter-subject anatomic variability and differences in maturation levels warrant the development and use of spatiotemporal atlases of the developing brain.

P. Golland et al. (Eds.): MICCAI 2014, Part II, LNCS 8674, pp. 292–299, 2014.

The construction of digital spatiotemporal MRI atlases of early brain development is relatively new. A 4D probabilistic atlas of early brain growth was developed in [10] through pairwise affine registration in space and kernel regression in time from MRI of 142 preterm infants in the 29 to 44 weeks term-equivalent gestational age (GA). A higher dimensional non-rigid registration approach based on Bspline free-form deformation (FFD) was used in [9], in which the authors showed marked improvements over the use of affine registration in spatiotemporal atlas construction. The first spatiotemporal probabilistic MRI atlas of the fetal brain was developed in [5] through kernel regression in time and affine registration of manually segmented fetal brain tissue in 20 healthy fetuses in the GA range of 20.57 to 24.71 weeks. More recently the atlas construction method in [9] was used to construct a probabilistic spatiotemporal atlas of the fetal brain in the GA range of 23 to 37 weeks.

As compared to the atlas construction methods reviewed above, which used either affine or FFD-based deformation models, we propose a new method based on diffeomorphic deformable registration where we integrate symmetric normalization in space [11] with kernel regression in time for spatiotemporal atlas construction. This topology-preserving approach generates unbiased sharp atlases of the population anatomy through kernel weighted averaging of deformation fields. Within our atlas construction framework we evaluate and compare the performance of mean square intensity difference (MSD), mutual information (MI), and cross correlation (CC) similarity metrics, and compare variants of FFD and Demons deformation models with symmetric diffeomorphic deformation. Evaluation of deformation models and similarity metrics for inter-subject brain MRI registration has been carried out in a number of previous studies including [12] and [13] which imply that CC or MI similarity metrics along with diffeomorphic deformation can be the best candidates; however whether those results are valid for inter-subject fetal brain MRI registration is yet to be investigated here too.

We emphasize that precise inter-subject registration not only leads to sharper atlases of the developing brain but also has a significant impact on the accuracy of atlas-based segmentation and group analysis studies. In Section 2 we start with the formulation of deformable registration and follow with the description of our atlas construction framework. Section 3 entails our experimental results which include the construction of a normative spatiotemporal atlas of the fetal brain in the third trimester from 40 normal fetuses in the GA range of 26 to 36 weeks, and our evaluations that show symmetric diffeomorphic deformation with CC similarity metric performs significantly better than other configurations in this application. Section 4 contains a brief discussion and the concluding remarks.

2 Methods

2.1 Pre-processing

Fetal brain MRI is performed through multiple single shot fast spin echo (SSFSE) scans in the orthogonal planes of the fetal brain. With this sequence all k-space samples of a 2D slice are collected in a few hundred milliseconds to freeze

the motion of the fetus at the instant of imaging. High-quality slices are typically achieved by this protocol in the presence of fetal and maternal motion; however, severe inter-slice motion artifacts, as shown in the left most picture in Figure 1, are seen in the out-of-plane views. Fetal MRI scans are thus preprocessed to correct for these artifacts through the steps shown in Figure 1. In order to compensate for the arbitrary orientation of the fetal brain MRI, prior to deformable registration for atlas construction, we bring all fetal brain MRI images into the same spatial location and orientation by using first order geometric moments followed by multi-scale mutual information based rigid registration [8].

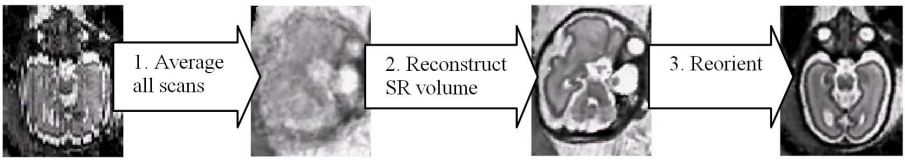

Fig. 1. The preprocessing steps in fetal brain MRI analysis: 1) an initial estimate of fetal brain volume is obtained by averaging original SSFSE scans, 2) a volumetric fetal brain MRI is reconstructed via iterations of inter-slice motion correction and volume reconstruction [2], and 3) the reconstructed image, which is arbitrarily oriented in the reference coordinate system, is reoriented to an orthogonal plane of the fetal brain by applying the inverse of the direction cosines matrix of the original scan [8].

2.2 Image Registration

We define image registration as the problem of finding a transformation $h_i : \Omega \to \Omega$, defined in the space of the underlying coordinate system $\Omega \subset R^3$, that matches dense correspondences between a source image $I_i(x) : R^3 \to R$ and a target image $I_T(x) : R^3 \to R$. In this formulation each image assigns an intensity value to each 3D point in Ω, and the transformation is applied to the source image through $I_i \circ h_i = I_i(h_i^{-1}(x))$ [14]. The transformation model can be rigid, affine, or deformable; but often a high-dimensional deformation model is needed to capture anatomic variability between subjects. Among various deformation models, we build our registration algorithm based on viscous fluid model and compare it to variants of FFD and Demons deformation models (see [12] for a review and comparison of methods).

Assuming a viscous fluid model the deformations are obtained from the solution of the Lagrangian ODEs [11]:

$$\frac{\mathrm{d}}{\mathrm{d}s} h_i(x,s) = v_i(h_i(x,s),s); \quad h_i(x,0) = h_0 \tag{1}$$

where $s \in [0,1]$ is a simulated time parameter, v_i are velocity fields, and h_0 is the initial (often identity) transformation. The deformations h_i are generated by integrating velocity fields forward in time and their inverse h_i^{-1} are generated

by integrating negative velocity fields backward in time. Integrating Equation 1 generates a diffeomorphism, which is by definition a differentiable map with differentiable inverse, and is thus topology-preserving.

We define the image registration cost function as:

$$E(I_T, I_i \circ h_i, h_i)^2 = Sim(I_i(h_i^{-1}(x)), I_T(x))^2 + D(\mathtt{Id}, h_i)^2 \tag{2}$$

where $Sim(.)$ is a similarity metric between two images, $\mathtt{Id}$ is the identity transform; and $D(\mathtt{Id}, h_i)^2$ is a squared distance metric which is defined as:

$$D(\mathtt{Id}, h_i)^2 = min_v \int_0^1 \int_\Omega \|Lv_i(x,s)\|^2 dxds \tag{3}$$

subject to $h_i(x) = x + \int_0^1 v_i(h_i(x,s),s)ds$; $L = \mu\nabla^2 + (\lambda+\mu)\overrightarrow{\nabla}(\overrightarrow{\nabla}.)$ is the Cauchy-Navier operator; and $\|.\|$ is the standard L^2 norm.

In this formulation the transformation is only applied to the source image, which results in asymmetric optimization and bias in atlas construction. In order to mitigate this effect we follow the symmetric normalization approach developed by Avants et al. in [15], in which the deformation h_i is split equally between the pair of images I_i and I_T. We use the open source ANTS software (http://picsl.upenn.edu/software/ants/) in implementation. Next we will show how we use this registration framework in spatiotemporal atlas construction.

2.3 Spatiotemporal Atlas Construction

A spatiotemporal template is an unbiased average representation of the anatomy as a function of time (age) and thus should effectively capture and encode the anatomic variability of the population in deformation fields. The geometric anatomic variability usually cannot be represented by elements of a Hilbert space and should instead be modeled by large deformations that belong to the high-dimensional group of diffeomorphisms ($\mathcal{H}$) [16]. In $\mathcal{H}$ the addition of two elements is not necessarily a diffeomorphism, therefore the linear averaging of deformation fields is not well defined. To address this problem we follow the minimum distance template estimation approach in [11,16,17] where we integrate kernel regression in age with diffeomorphic mapping in space in our formulation.

Given a collection of M images $I_i(x)$ acquired at the corresponding ages τ_i from individuals in a population, the problem is formulated as finding a set of transformations $h_{i,\tau} \in \mathcal{H}$ and a template $\bar{I}_\tau$ that is a minimum distance representation of the population anatomy at age τ. We write this as the following minimization problem:

$$\hat{h}_{i,\tau} = argmin_{h_{i,\tau}} \Sigma_{i=1}^{M} C_{\tau,\tau_i} E(\bar{I}_\tau, I_i, h_{i,\tau})^2 \tag{4}$$

where C_{τ,τ_i} are non-negative sum-of-unity coefficients that incorporate kernel regression in time, and $E(\bar{I}_\tau, I_i, h_{i,\tau})^2$ is the cost function defined by replacing I_T with $\bar{I}(\tau)$ in Equation 2. The outcome of this minimization problem is a set of M deformation fields $h_{i,\tau}$ and an unbiased average template $\bar{I}_\tau$ at age τ.

We solve this minimization problem through a numerical approach based on the variation of the desired velocity fields v_i^* through an iterative algorithm:

1. For each simulated time s, initialize $v_{i,\tau} = \texttt{Id}$;
2. For $i = 1...M$ solve $v_{i,\tau}^*(x) = argmin_{v_{i,\tau}(x)} E(\bar{I}_\tau, I_i, h_{i,\tau})^2$
3. Set optimal $\bar{v}_\tau^*(x)$ as

$$\bar{v}_\tau^*(x) = \frac{1}{\Sigma_{i=1^M} \mathbf{K}(\tau - \tau_i)} \Sigma_{i=1}^{M} \mathbf{K}(\tau - \tau_i) v_{i,\tau}^*(x) \tag{5}$$

where $K(.)$ is a kernel function.

4. Find the new $\bar{h}_\tau(x)$ based on $\bar{v}_\tau(x)$
5. Repeat until $\bar{h}_\tau(x)$ converges and $\bar{I}_\tau$ is obtained.

The algorithm starts with a weighted average of the anatomy based on kernel regression and then flows towards a mean representation of the anatomy at any given age τ which typically converges in 5 to 10 iterations. For the similarity function $Sim(.)$ defined in Equation 2 we used and compared MSD, MI, and CC similarity metrics; and compared the performance of diffeomorphic deformation with variants of FFD and Demons deformation fields.

3 Results

We tested our atlas construction method based on fetal MRI of 40 healthy fetuses from 26.14 to 35.86 weeks GA (mean=30.50, stdev=3.05). Imaging was performed on a 1.5-T scanner (Achiva, Philips Medical System, Netherlands) and a 5-channel phased-array cardiac coil. Multi-planar SSFSE scans were performed with effective echo time of 120 ms, repetition time of 12500 ms, 0.625 signal averages, 330-mm field of view, 2-mm slice thickness, no inter-slice gap, and 256x204 acquisition matrix, acquisition time 30 to 60 seconds).

Volumetric fetal brain MRI was reconstructed for all fetuses with an isotropic resolution of 1mm in 3D using super-resolution volume reconstruction [2]. The images were pre-processed by the steps discussed in Section 2.1. The processed images were then used for spatiotemporal atlas construction as discussed in Section 2. Figure 2 shows five exemplary age points of our constructed spatiotemporal fetal brain MRI atlas. Note that with the algorithm we described an average atlas can be obtained at any given continuous age point. The atlas is available online at typical age points: crl.med.harvard.edu/research/fetal_brain_atlas/

For quantitave evaluation we calculated two monotonic and robust-to-noise sharpness measures, i.e. M1 (the intensity variance measure) and M2 (the energy of image gradient measure), on atlases, and confirmed the results with visual inspection. First we examined and compared three similarity metrics, i.e. MSD, MI, and CC. The results showed that CC performed significantly better than MSD and MI. Then, with CC as the similarity metric, we compared our suggested method based on diffeomorphic deformation model with variants of FFD and Demons deformation models. As typical representatives of all results Fig. 3

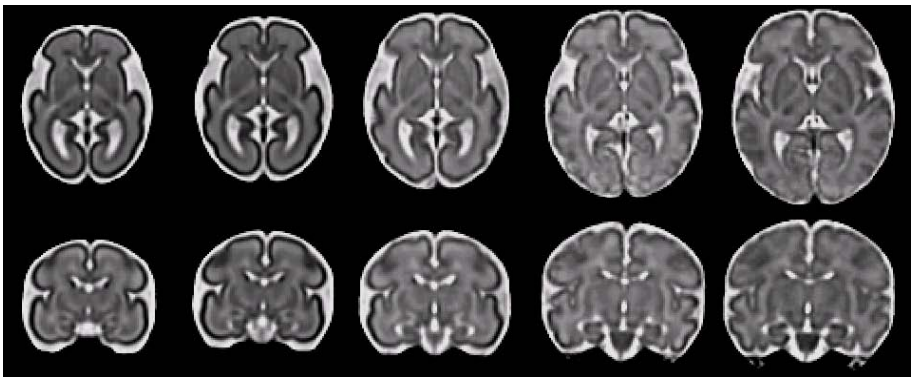

Fig. 2. Five age points of the generated spatiotemporal fetal brain MRI atlas (at 27, 29, 31, 33, and 35 weeks GA). We used CC similarity metric to generate this atlas.

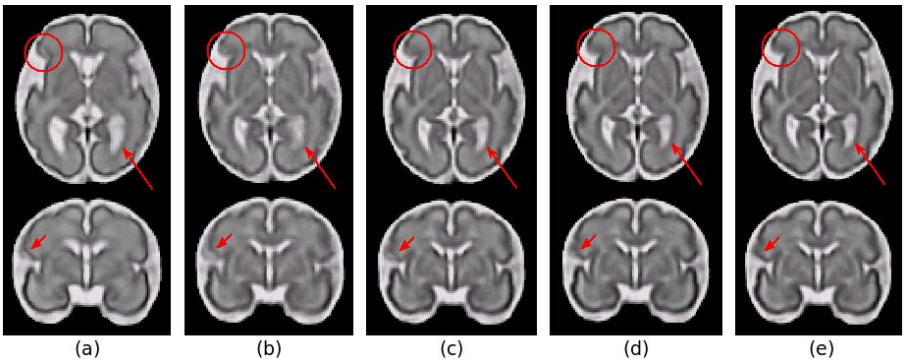

Fig. 3. Visual comparison of atlases constructed using (a) MSD and (b) MI similarity metrics (with diffeomorphic deformation), and (c) Demons, (d) FFD, and (e) symmetric diffeomorphic deformation models with CC similarity metric. Arrows and circles highlight some of the most prominent visual differences, which show that our proposed method performed best with CC similarity metric, whereas other configurations and MSD and MI did not successfully capture inter-subject anatomic variability.

compares the constructed atlases at 31 week GA and Fig. 4 shows a comparison of sharpness measures normalized in each group for 27 and 35 weeks GA points.

To see if a statistically significant difference is detected by sharpness measures (nM1 and nM2) between the methods, we used analysis of variance (ANOVA) with Bonferroni correction on 45 samples from 5 groups, and pairwise comparison with paired two sample t-tests. A statistically significant difference was detected by ANOVA and the t-tests. Table 1 shows adjusted p values for the pairwise comparisons between our suggested method (CC) and four other methods.

Table 1. Adjusted p values for the pairwise comparison of nM1 and nM2 sharpness measures between CC and four other methods: Our suggested method based on symmetric diffeomorphic deformation and CC similarity metric generated significantly sharper atlas than all other methods according to both sharpness measures.

nM1	MI	MSD	Demons	FFD	nM2	MI	MSD	Demons	FFD
	$< 10^{-6}$	$< 10^{-4}$	< 0.0005	< 0.001		$< 10^{-6}$	$< 10^{-6}$	$< 10^{-4}$	< 0.0005

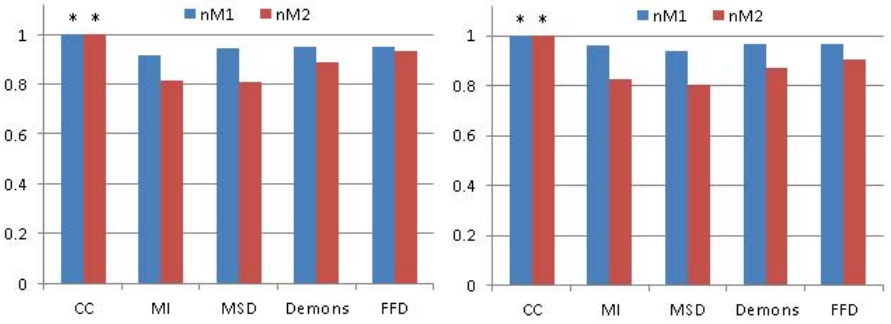

Fig. 4. Normalized sharpness measures (nM1 and nM2) calculated for 5 atlas construction methods at 2 GA points (27 week on left & 35 week on right). Similar results obtained for all atlases showed that diffeomorphic deformation with CC similarity metric consistently generated the sharpest atlases among all methods for all gestation ages.

4 Conclusion

We developed an algorithm for automatic construction of deformable spatiotemporal atlases of the fetal brain. Within this framework we examined the performance of atlas construction based on different registration parameters through calculating two robust sharpness measures and confirmed with visual inspection. The results indicate that the formulation we developed based on symmetric diffeomorphic deformation and CC similarity metric integrated with kernel regression in age, performed significantly better than alternative configurations. We therefore suggest the use of symmetric diffeomorphic deformable registration for inter-subject fetal brain MRI registration and this approach for deformable atlas construction and atlas-based segmentation.

Acknowledgments. This study was supported in part by NIH grants R01 EB013248, R01 RR021885, R03 DE22109; the Thrasher Research Fund; and in part by Harvard Catalyst - Harvard Clinical and Translational Science Center for Research Resources and the National Center for Advancing Translational Sciences, NIH award 8KL2TR000168-05. The authors also acknowledge the funding by the Canadian Institute of Health Research (C. Limperopoulos: MOP 81116).

References

1. Studholme, C.: Mapping fetal brain development in utero using magnetic resonance imaging: The big bang of brain mapping. Annual Review of Biomedical Engineering 13, 345–368 (2011)
2. Gholipour, A., Estroff, J., Warfield, S.: Robust super-resolution volume reconstruction from slice acquisitions: application to fetal brain MRI. IEEE Transactions on Medical Imaging 29(10), 1739–1758 (2010)
3. Kuklisova-Murgasova, M., Quaghebeur, G., Rutherford, M.A., Hajnal, J.V., Schnabel, J.A.: Reconstruction of fetal brain MRI with intensity matching and complete outlier removal. Medical Image Analysis 16(8), 1550–1564 (2012)
4. Habas, P.A., Kim, K., Rousseau, F., Glenn, O.A., Barkovich, A.J., Studholme, C.: Atlas-based segmentation of developing tissues in the human brain with quantitative validation in young fetuses. Human Brain Mapping 31(9), 1348–1358 (2010)
5. Habas, P., Kim, K., Corbett-Detig, J., Rousseau, F., Glenn, O., Barkovich, A., Studholme, C.: A spatiotemporal atlas of MR intensity, tissue probability and shape of the fetal brain. Neuroimage 53(2), 460–470 (2010)
6. Rajagopalan, V., Scott, J., Habas, P., Kim, K., Corbett-Detig, J., et al.: Local tissue growth patterns underlying normal fetal human brain gyrification quantified in utero. The Journal of Neuroscience 31(8), 2878–2887 (2011)
7. Clouchoux, C., Kudelski, D., Gholipour, A., Warfield, S.K., Viseur, S., Bouyssi-Kobar, M., Mari, J.L., Evans, A.C., du Plessis, A.J., Limperopoulos, C.: Quantitative in vivo MRI measurement of cortical development in the fetus. Brain Structure and Function 217(1), 127–139 (2012)
8. Gholipour, A., Akhondi-Asl, A., Estroff, J.A., Warfield, S.K.: Multi-atlas multi-shape segmentation of fetal brain MRI for volumetric and morphometric analysis of ventriculomegaly. NeuroImage 60(3), 1819–1831 (2012)
9. Serag, A., Aljabar, P., Ball, G., Counsell, S.J., Boardman, J.P., Rutherford, M.A., Edwards, A.D., Hajnal, J.V., Rueckert, D.: Construction of a consistent high-definition spatio-temporal atlas of the developing brain using adaptive kernel regression. NeuroImage 59(3), 2255–2265 (2012)
10. Kuklisova-Murgasova, M., Aljabar, P., et al.: A dynamic 4D probabilistic atlas of the developing brain. NeuroImage 54(4), 2750–2763 (2011)
11. Avants, B., Gee, J.: Geodesic estimation for large deformation anatomical shape averaging and interpolation. NeuroImage 23, S139–S150 (2004)
12. Klein, A., Andersson, J., Ardekani, B.A., Ashburner, J., Avants, B., et al.: Evaluation of 14 nonlinear deformation algorithms applied to human brain MRI registration. Neuroimage 46(3), 786–802 (2009)
13. Avants, B.B., Tustison, N.J., Song, G., Cook, P.A., Klein, A., Gee, J.C.: A reproducible evaluation of ANTs similarity metric performance in brain image registration. Neuroimage 54(3), 2033–2044 (2011)
14. Gholipour, A., Kehtarnavaz, N., Briggs, R., Devous, M., Gopinath, K.: Brain functional localization: a survey of image registration techniques. IEEE Transactions on Medical Imaging 26(4), 427–451 (2007)
15. Avants, B., Epstein, C., Grossman, M., Gee, J.: Symmetric diffeomorphic image registration with cross-correlation: Evaluating automated labeling of elderly and neurodegenerative brain. Medical Image Analysis 12(1), 26 (2008)
16. Joshi, S., Davis, B., Jomier, M., Gerig, G.: Unbiased diffeomorphic atlas construction for computational anatomy. NeuroImage 23, S151–S160 (2004)
17. Davis, B., Fletcher, P., Bullitt, E., Joshi, S.: Population shape regression from random design data. Int. Journal of Computer Vision 90(2), 255–266 (2010)